The Journal of Chemical Physics

Dynamical properties of a room temperature ionic liquid: Using molecular dynamics simulations to implement a dynamic ion cage model

Cite as: J. Chem. Phys. **151**, 154502 (2019); https://doi.org/10.1063/1.5126231
Submitted: 30 August 2019 . Accepted: 16 September 2019 . Published Online: 18 October 2019

Maolin Sha, Xiaohang Ma, Na Li, Fabao Luo, Guanglai Zhu, and Michael D. Fayer

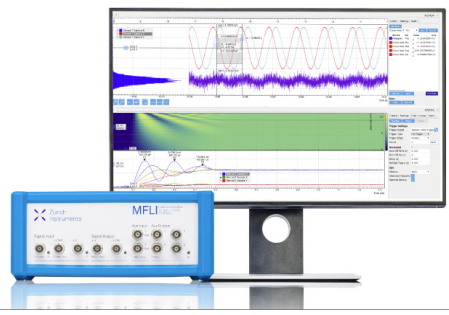

The Journal of Chemical Physics ARTICLE scitation.org/journal/jcp

Dynamical properties of a room temperature ionic liquid: Using molecular dynamics simulations to implement a dynamic ion cage model

Cite as: J. Chem. Phys. 151, 154502 (2019); doi: 10.1063/1.5126231
Submitted: 30 August 2019 • Accepted: 16 September 2019 •
Published Online: 18 October 2019

Maolin Sha,[1,2,a)] Xiaohang Ma,[1] Na Li,[3] Fabao Luo,[3] Guanglai Zhu,[4] and Michael D. Fayer[2,a)]

AFFILIATIONS

[1]Department of Physics and Materials Engineering, Hefei Normal University, Hefei 230061, China
[2]Department of Chemistry, Stanford University, Stanford, California 94305, USA
[3]Department of Chemistry and Chemical Engineering, Hefei Normal University, Hefei 230061, China
[4]Institute of Atomic and Molecular Physics, Anhui Normal University, Wuhu 241000, China

[a)]**Electronic addresses:** franksha@aliyun.com and fayer@stanford.edu. **Telephone:** 650 723-4446.

ABSTRACT

The transport behavior of ionic liquids (ILs) is pivotal for a variety of applications, especially when ILs are used as electrolytes. Many aspects of the transport dynamics of ILs remain to be understood. Here, a common ionic liquid, 1-butyl-3-methylimidazolium bis(trifluoromethylsulfonyl)imide ($BmimNTf_2$), was studied with molecular dynamics simulations. The results show that $BmimNTf_2$ displays typical structural relaxation, subdiffusive behavior, and a breakdown of the Stokes-Einstein diffusion relation as in glass-forming liquids. In addition, the simulations show that the translational dynamics, reorientation dynamics, and structural relaxation dynamics are well described by the Vogel-Fulcher-Tammann equation like fragile glass forming liquids. Building on previous work that employed ion cage models, it was found that the diffusion dynamics of the cations and anions were well described by a hopping process random walk where the step time is the ion cage lifetime obtained from the cage correlation function. Detailed analysis of the ion cage structures indicated that the electrostatic potential energy of the ion cage dominates the diffusion dynamics of the caged ion. The ion orientational relaxation dynamics showed that ion reorientation is a necessary step for ion cage restructuring. The dynamic ion cage model description of ion diffusion presented here may have implications for designing ILs to control their transport behavior.

I. INTRODUCTION

Room temperature ionic liquids (ILs) have attracted substantial interest in recent decades.[1–3] Their special physicochemical properties, e.g., the ability to solvate a wide range of molecules, large electrochemical window, high thermal stability and conductivity, negligible vapor pressure, and low melting temperature, make them suitable candidates in various applications, including synthesis, separations, electrochemistry, catalysis, batteries, and supercapacitors.[4–10] Another advantage of ILs is the facile tunability of their physicochemical properties by employing different cation and anion combinations. Hence, ILs are commonly called designer liquids or task-specific ILs.

In applications, ILs' basic physicochemical properties are important, especially their dynamic properties. However, after nearly 20 years of study, there are still many unanswered questions, contradictions, and uncertain mechanisms regarding the transport dynamics of ILs.[11] For example, a number of studies have pointed out that IL viscosities and diffusion constants follow the Vogel-Fulcher-Tammann (VFT) equation $A(T) = A_0 \exp(\frac{B}{T-T_0})$ as in fragile glass forming liquids.[12–14] However, there are also reports indicating that the transport behavior of ILs follow an Arrhenius relationship over a range of temperatures.[15,16] The formation of ion pairs and ion clusters in ionic liquid microstructure and dynamics is another active topic.[17–20] What are the underlying physical mechanisms controlling IL transport dynamics and the formation of ion pairs and clusters? Which model can better depict transport in ILs, Debye-Hückel theory, cooperative ion motions, or ion pair models? These questions remain unanswered. Moreover, recent

studies confirmed that structural and dynamical heterogeneities are common phenomena in ionic liquids.[21–25] These results add complexity to understanding the transport dynamics of ionic liquids because structural and dynamical heterogeneities are common properties of glass-forming or supercooled liquids.[26–30]

To address ion transport in IL, we first need to understand the complicated interactions in ILs themselves. There are complex Coulomb, van der Waals, and hydrogen bonding interactions within the ionic liquid system. The complex hydrogen bonding interactions are close to those found in water or other multihydrogen bonding systems. The strong Coulomb interactions are similar to those observed in high-temperature molten salts. The van der Waals and dispersion interactions are analogous to those found for large organic molecules. This diversity of interactions complicates efforts to understand transport dynamics in ILs.

Recently, there have been qualitative reports from molecular dynamics simulations and NMR experiments that the translational dynamics of ILs may exhibit subdiffusive behavior and nonexponential relaxations.[31,32] Gebbie *et al.*[33] pointed out that most ions are bound as ion pairs and behave effectively as dipoles. The IL transport dynamics depend heavily on a few free ions forming a dilute electrolyte. However, other work suggests that ion pairs have a short lifetime, and the ILs may behave as concentrated electrolytes.[34–36] Several experiments confirmed that both ion pairs and ion clusters exist in IL systems.[37,38] Maginn *et al.*[39,40] invoked an ion cage model and calculated the dynamics properties of 29 ILs. Their results indicated a linear relationship between the translational dynamics and long ion pair or ion cage lifetimes. Their excellent works demonstrated that the local microstructure of ILs can be directly related to the dynamic properties.

Here, we made use of molecular dynamics simulations to study dynamics, particularly ion transport, in the common ionic liquid, 1-butyl-3-methylimidazolium bis(trifluoromethylsulfonyl)imide BmimNTf$_2$ (see the supplementary material for the molecular structure). The results extend the prior ion cage model research by using the cage correlation function to obtain a jump time that becomes the step time in a random walk determination of the cation and anion diffusion constants. The diffusion constants obtained from the random walk model are in quantitative agreement with the diffusion constants found directly from the simulations. Other aspects of the ion cages are presented, such as cage structure distributions as a function of temperature.

II. SIMULATION DETAILS

The BmimNTf$_2$ was treated with a systematic all-atom force field, as developed by Köddermann *et al.*[41] The force field has been shown to provide a much better description of transport properties without resorting to the typical method of charge scaling. It has also been used successfully in previous simulations[42,43] and can reproduce the structural and dynamical properties of imidazolium-based ionic liquids in experiments. Figures S1 and S2 display the temperature-dependent mass densities and diffusion coefficients of the IL BmimNTf$_2$ from our simulations with comparison to the experiments (see the supplementary material). We also calculated the translational and rotational dynamics using a polarizable force field[44] and compared the results to the force field used here in Figs. S3 and S4. These comparisons validate that the nonpolarizable force field used in this study can accurately simulate the structural and dynamic properties of the IL BmimNTf$_2$.

The model system consists of 512 BmimNTf$_2$ molecules placed in a tetragonal box. The cross interactions between unlike atoms were computed according to the Lorentz-Berthelot combination rules. The series of simulations were performed by using Gromacs 5.0.[45–47] 17 ionic liquid systems with different temperatures ranging from 240 K to 400 K were studied. The simulations were initially equilibrated at an isothermal-isobaric condition (NPT) at 1 atm for 5 ns. The systems were then further equilibrated in a constant volume-temperature (NVT) ensemble for 10 ns. Trajectories of an additional 30 ns following equilibration were used for dynamic analysis.

Periodic boundary conditions were applied in all directions. In all simulations, the bond length was constrained with the LINCS algorithm. The cutoff of Lennard-Jones interactions was taken 12 Å. The long-range coulomb interactions were treated by PME with a cutoff of 12 Å and a grid spacing of 1.2 Å. The Berendsen thermostat and a velocity rescaling thermostat were separately used in the NPT and NVT systems, respectively, to mimic the weak coupling with a temperature coupling constant of 0.1 ps.

III. RESULTS AND DISCUSSION

A. Self-intermediate scattering function

The self-intermediate scattering function (ISF),[48,49] $F_s(\vec{k},t)$, which is defined by $F_s\left(\vec{k},t\right) = \frac{1}{N}e\left\langle -i\vec{k}\left[\vec{r_i}(t) - \vec{r_i}(0)\right]\right\rangle$, is frequently applied in various glasses or supercooled liquids for analyzing structural relaxation. Figure 1 displays $F_s(\vec{k},t)$ in a wide range of temperatures from 240 K to 400 K. The ISFs decay as in a normal liquid when the temperature is high. When the temperature decreases, the curves exhibit an intermediate plateau regime (β-relaxation) and an α-relaxation regime, as seen in glass-forming liquids.[50] However, these temperatures are well above the glass transition temperature (181 K) of the IL BmimNTf$_2$. Both the ISFs of the cation and the anion show similar behavior, i.e., a characteristic two-step signature of glass-forming liquids upon cooling. Based on mode coupling theory, a very short-time decay due to librational dynamics is followed by a long-time decay caused by structural relaxation.[51] This very similar behavior, especially in the long time decay for the cations and the anions, means that the coupling of long range motion of the cations and the anions is very significant.

We define the structural relaxation time τ as the time after which the ISF has decayed from 1 to 1/e. The classic hydrodynamics model requires that the diffusion of particles abide by the Stokes-Einstein relation. However, the fractional Stokes-Einstein relation[52] is commonly used to describe the behavior of glass-forming liquids. The fractional Stokes-Einstein relation is $D\cdot(\tau/T)^{\gamma} = C$, where D is the diffusion coefficient and C is a constant. If $\gamma \neq 1$, a breakdown of the classical Stokes-Einstein relation occurs. Figure 2 shows log plots of the self-diffusion coefficients and the structural relaxation times for the cations and the anions. We obtain γ values of 0.832 and 0.830 for the cation and the anion, respectively. This fractional Stokes-Einstein relation reconfirms the subdiffusive behavior and the glass-forming liquid dynamics in the IL. This breakdown

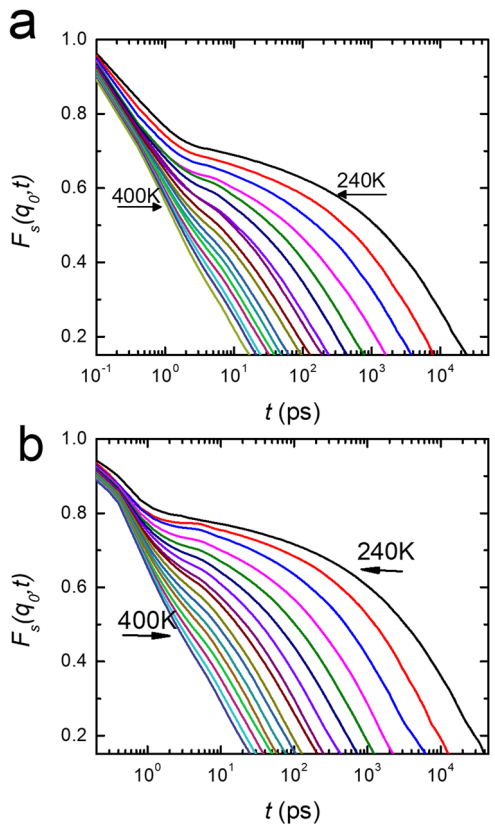

FIG. 1. Self-intermediate scattering function $Fs(q_0,t)$ for (a) cations and (b) anions. The wave vector q_0 is set to 1.256 Å^{-1}, which corresponds to the first nearest neighboring position for all ions.

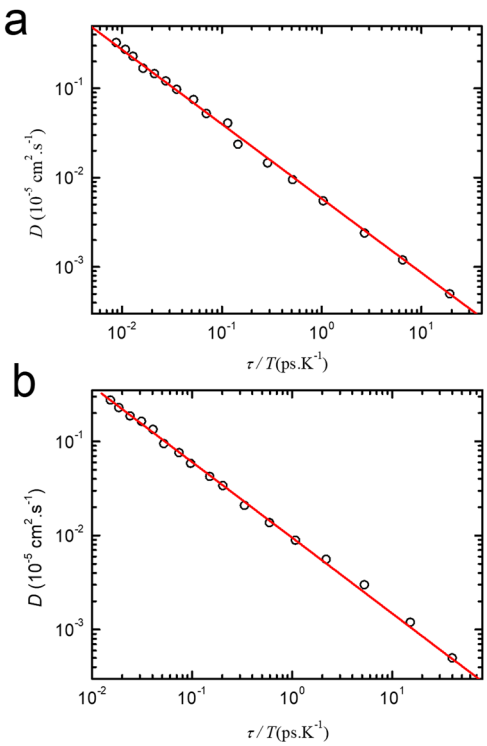

FIG. 2. The log-log relation between the self-diffusion coefficients and the structural relaxation time for (a) cations and (b) anions. The structural relaxation time is the time after which the ISF has decayed from 1 to 1/e.

of the Stokes-Einstein relation has already been found in experiments and other simulations for other ILs.[42,43] The results also demonstrate that the translational dynamics of the ionic liquid cannot be described by the conventional diffusion equation, which is a continuity equation combined with a constitutive relation given by Fick's law.[42,43]

The breakdown of the classic Stokes-Einstein relation is usually related to the liquid "fragility" and the dynamical heterogeneity. Angell[53] proposed "fragile" or "strong" to describe glass-forming liquids. ILs are usually considered "fragile" liquids because their dynamic properties deviate from Arrhenius behavior. Figure 3 shows the temperature-dependent structural relaxation time for the cation and the anion. For both the cation and the anion, we observe that the data are reasonably well described by a fit to the VFT equation, showing typical "fragile" behavior. In Fig. 3, we can also fit an Arrhenius equation for the high temperature region. The deviation from Arrhenius behavior begins at ~300 K, which is somewhat higher than the melting point of $BmimNTf_2$, 269 K. It means that this fragile property not only holds at supercooled temperatures but also persists even at 400 K, which is much higher than the melting point of the IL $BmimNTf_2$. This result demonstrates that the normal liquid state IL still presents a "fragile" property, like glass-forming or supercooled liquids.

B. Cage dynamics

Berne and co-workers[54,55] proposed a cage hopping model to describe diffusion in molecular liquids. They developed a cage correlation function to explicate the diffusion behavior of this hopping process. ILs consist of cations and anions. Due to the strong Coulomb interactions between the cations and anions, ILs likely form complex ion cages or ion cluster structures. Whether ion pairs or ion clusters are stable in ILs is controversial.[35,36] Recent experiments demonstrated the subdiffusive behavior of ILs.[32] The radial distribution functions of ILs also show that the ions in IL systems are surrounded by several counterions to form an oppositely charged ion shell (see below). This ion shell structure or ion cage may determine the ion diffusion properties.

The idea of the cage correlation function is illustrated in Fig. 4. The cage correlation function can be defined as $C_{cage}^{out}(t) \equiv \left\langle \Theta\left(c - n_i^{out}(0,t)\right)\right\rangle$, where Θ is the Heaviside step function, c is the number of molecules that must leave a particular molecule's neighbor list before it is reasonable to consider that a change in the surroundings has taken place.[54,55] Here, we have chosen $c = 1$. n_i^{out} is the number of molecules that have left molecule i's original neighbor list at time t, $n_i^{out}(0,t) = |l_i(0)|^2 - l_i(0) \cdot l_i(t)$. $l_i(t)$ is molecule i's neighbor list at time t. $l_i(t)$ can be written as $l_i \equiv \begin{pmatrix} f(r_{i1}) \\ \cdots \\ f(r_{iN}) \end{pmatrix}$, where $f(r_{ij})$ is a function of the intermolecular

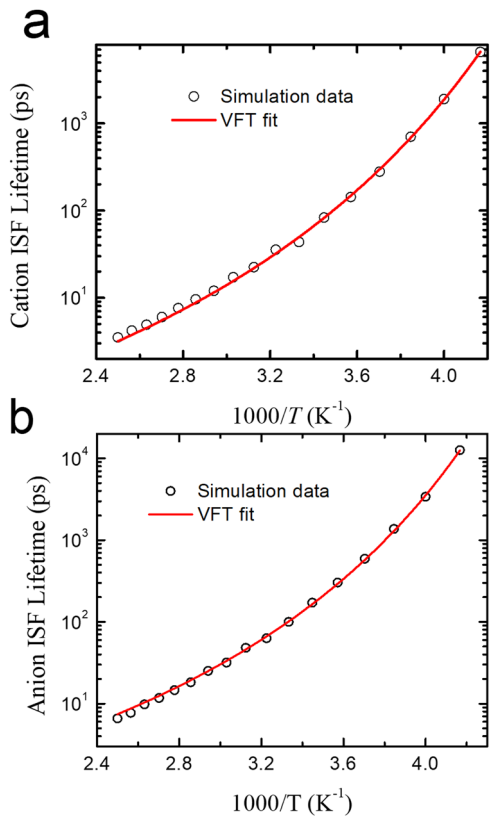

FIG. 3. Temperature-dependent structural relaxation time for (a) cations and (b) anions. The simulation data were fitted by the VFT equation (solid lines).

distances. Typically, $f(r_{ij})$ is the Heaviside step function as $f(r_{ij}) = \Theta(r_{\min} - r_{ij}) = \begin{cases} 1 \; if & r_{ij} \le r_{\min} \\ 0 & otherwise \end{cases}$, where $r_{\min}$ is the neighbor list cutoff radius. In calculating C_{cage}, we set $r_{\min}$ to the location of the minimum in the cation-anion radial distribution function $g(r)$ (see below). Here, we calculated the temperature-dependent cage correlation functions of the cation and anion, as shown in Fig. 5. Both the cation and the anion display a

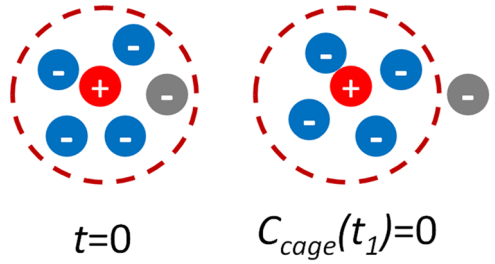

FIG. 4. A sketch of the cage correlation function. The cage radius is denoted by the dotted line. The gray anion was inside the red cation's cage at time 0 (left side), but has exited the cage at time t_1 (right side). The value of the cage correlation function, C_{cage}, is therefore 0 even though the original 4 anions stayed within the cage radius.

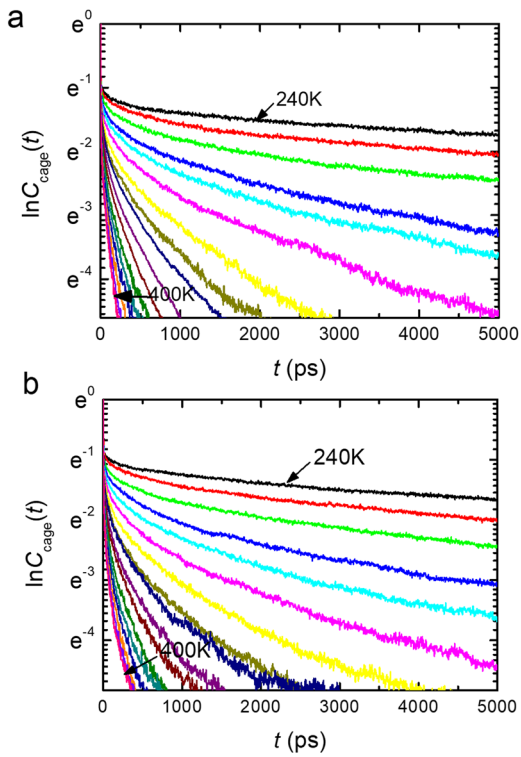

FIG. 5. A temperature-dependent center-of-mass cage correlation function for (a) cations and (b) anions.

fast decay of the cage correlation function (fast hopping process) at high temperature like normal liquids. At high temperatures, the decay times are tens to a hundred picoseconds. At lower temperatures, the cage dynamics slow dramatically to many nanoseconds.

Figure 6 shows a direct relationship between the diffusion coefficients and the inverse of cage lifetimes, $1/\tau_c$, for the cation and the anion. τ_c for each temperature is the integral of the curves, $C_{\text{cage}}(t)$ shown in Fig. 5. τ_c is an average over the nonexponential $C_{\text{cage}}(t)$;

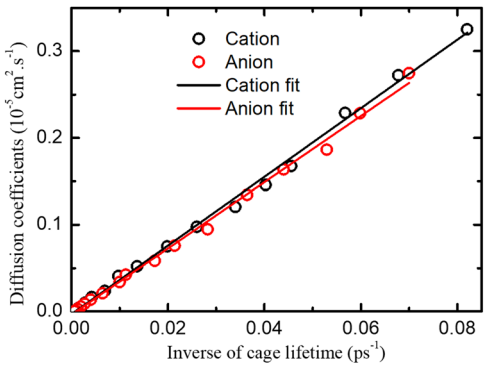

FIG. 6. Linear relations between the diffusion coefficients and the cage lifetimes for the cations and the anions, respectively.

it is the integral of the amplitude weighted decay time scales. The diffusion coefficients in Fig. 6 were obtained from the MD simulation trajectories of the ion displacements. The linear relationship between the diffusion coefficients and $1/\tau_c$ obtained from the cage correlation function confirms that ion diffusion is determined by ion cage dynamics. Consistent with the model, the jump process from one ion cage to another is the intrinsic physical mechanism governing the diffusion of ions in IL systems. NMR and quasielastic neutron scattering experiments[13,56] also suggest a hopping process. Maginn and Zhang[39] attributed this jump process to the association of ion pairs. Here, we expanded the idea in terms of random walk ion cages.

Due to the direct relationship between the cage lifetimes and the diffusion coefficients shown in Fig. 6, we can take the cage lifetime, τ_c, as the jump time in the hopping process. We can use a simple random walk model as another way of calculating the diffusion coefficients, but now using the cage correlation function results in the form of τ_c as the step time in the random walk. The diffusion coefficient, $D_c(t)$, obtained using τ_c employs the standard relation between the diffusion coefficient and a random walk on a lattice, $D_c = \sigma^2/(6\tau_c)$. σ is the random walk step size. The value of σ = 0.16 nm, obtained from the slope of the lines in Fig. 6, is very close to the hopping distance of 0.17 nm found in an NMR experiment on the same imidazolium cation.[13] Figure 7 shows a comparison of $D(t)$ obtained from the MD simulation trajectories and $D_c(t)$ obtained from the random walk model. There is one adjustable parameter, σ. The value of σ = 0.16 nm gives the best agreement between $D(t)$ and $D_c(t)$. Within the noise associated with the simulations, the agreement is extremely good. It is remarkable that a random walk on a lattice model can yield the correct diffusion coefficients when the integrals of the cage correlation function decays are used for the step times.

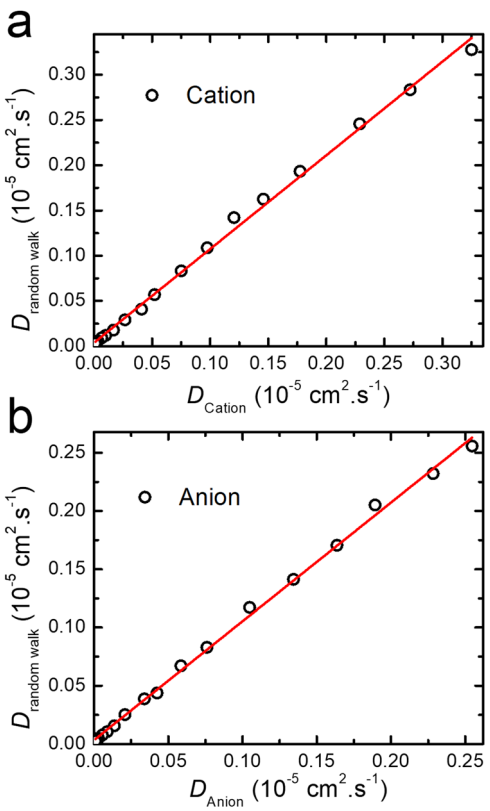

FIG. 7. The diffusion coefficients calculated by the mean square displacement and fit by the random walk model. Here τ is the hopping time in the ion cage. We set σ = 0.16 nm to fit the diffusion coefficients.

Maginn and Morrow[57] suggested that diffusion dynamics could be modeled as a hopping process. However, they did not obtain the correct diffusion coefficients from the random walk model, probably due to a deficiency of their force field parameters in the simulations of the IL dynamics. Here, the results shown in Figs. 6 and 7 provide strong support for ion cage random hopping as the mechanism that dominates diffusion dynamics. In general, diffusion is directly connected to the viscosity. Hence, very viscous ILs may result from ion cage structures with slowly decaying cage correlation functions. It may be possible to design ILs with particular diffusion dynamics by simulating the cage correlation functions for different anion and cation pairs without having to synthesize and test a large variety of pairs. Such an approach might be a useful strategy to find ILs with fast diffusion dynamics for use as electrolytes.

C. Subdiffusive behavior and reorientation dynamics

Supercooled liquids usually exhibit subdiffusive behavior.[58] Previously, subdiffusive behavior has been found in ILs in several experiments and MD simulations.[31,32] We also observe subdiffusive behavior of the ions of $BmimNTf_2$ as shown in Fig. S5 of the supplementary material. The mean square displacement (MSD) increases linearly in time, t, if the transport is diffusive. The MSD is a power law in t with an exponent of one. None diffusive behavior is manifested as an exponent less than one, with the exponent becoming one at sufficiently long time (see Fig. S5). At times less than a few picoseconds, the MSD increases with an apparent exponent of greater than one, as has been found in previous simulations.[31,32] It may be considered to be a ballistic regime. The diffusion dynamics observed in the simulations of $BmimNTf_2$ are analogous to the dynamics of glass-forming liquids. We also display the temperature-dependent diffusion coefficients in Fig. 8. Like the structural relaxation times (Fig. 3), the diffusion coefficients can be fit well by the VFT equation, showing typical glass-forming liquid character.

ILs exhibit complex interactions among different cations and anions. Hence, the reorientation dynamics of the ions in ILs are usually complicated and slow. We used the rotational autocorrelation function (ACF) to investigate the orientational dynamics of ILs. Here, we employed the first order Legendre polynomial orientational correlation function defined as $C_1(t) = \langle P_1(\cos\theta(t))P_1(\cos\theta(0))\rangle$, where $P_1(\cos\theta) = \cos\theta$. Figure S6 (supplementary material) displays the rotational ACF of the cation and anion. The decays are highly nonexponential. To characterize the orientational relaxation as a function of temperature, the curves in Figure S6 were integrated to give the characteristic orientational relaxation decay time, τ_R. At low temperatures, both the cations and anions exhibit very slow rotational dynamics, with τ_R greater than a nanosecond. Figure 9 displays the temperature dependence of τ_R for cations (a) and anions (b). Like translational

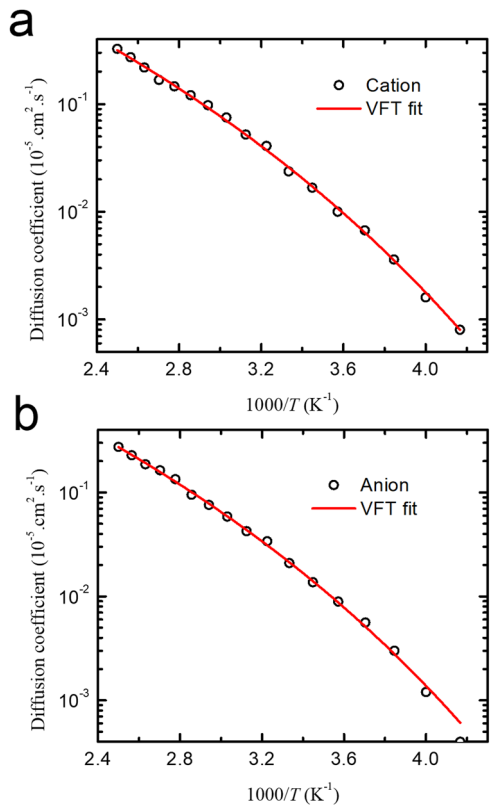

FIG. 8. The temperature-dependent diffusion coefficients for (a) cations and (b) anions. The solid line is the VFT fit of simulation data.

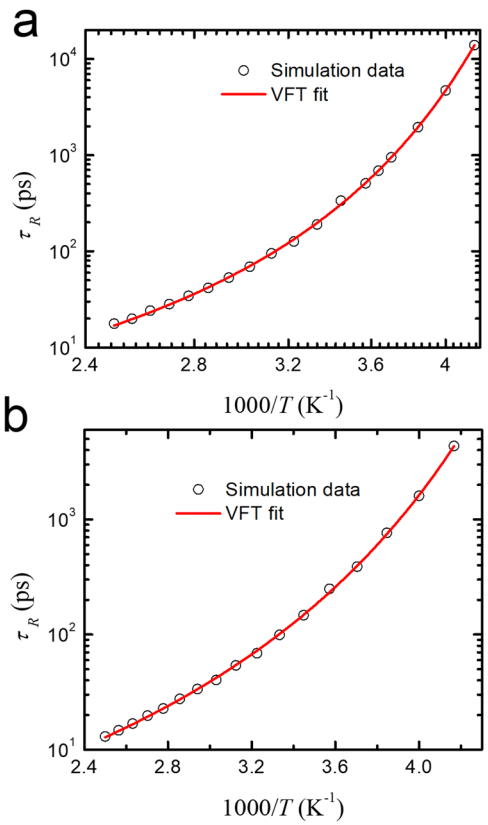

FIG. 9. The temperature-dependent rotational relaxation time for (a) the normal direction to the cation imidazolium ring and (b) the S-S vector in the anion.

diffusion and structural relaxation, the orientational relaxation dynamics can be fit with the VFT equation.

The values of the orientational relaxation decay times as a function of temperature are very close to the cage lifetimes discussed in detail above. Figure 10 displays the relationship between $1/\tau_R$ and the diffusion coefficient as a function of temperature. The linear relationship demonstrates strong coupling between the orientational dynamics and the translational dynamics. It is well-known that the diffusion coefficient is inversely proportional to the viscosity by the classic Stokes-Einstein relation. Hence, it appears that the orientation relaxation decay times are proportional to the viscosities as well. Several experiments[59,60] obtained similar results and concluded that the ILs should obey the hydrodynamics model, i.e., the Stoke-Einstein-Debye (SED) equation for orientational relaxation.

We can calculate the hydrodynamic volume of the molecule based on the hydrodynamic model. In the hydrodynamic model, the orientational relaxation time can be related to the viscosity via the generalized Stokes-Einstein-Debye (SED) equation, $\tau_{R2} = \frac{\eta(T)V\lambda}{6k_BT}$, where τ_{R2} is the orientational relaxation time from analysis using the second Legendre polynomial orientational correlation function C_2 (note $3\tau_R = \tau_{R2}$), η is the dynamic viscosity of the IL, V is the hydrodynamic volume, k_B is Boltzmann's constant, T is the absolute temperature, and λ is a friction coefficient that can be determined from the boundary conditions and molecular shape of the rotator.[61] The λ value is a dimensionless and is a function of the ratio, ρ, of the short to long semiaxes of the oblate or prolate spheroid for a slip boundary condition. Here, the cation was modeled as a prolate spheroid. Calculation of the λ value and the hydrodynamic volume are presented in the supplementary material. At 300 K, the calculated

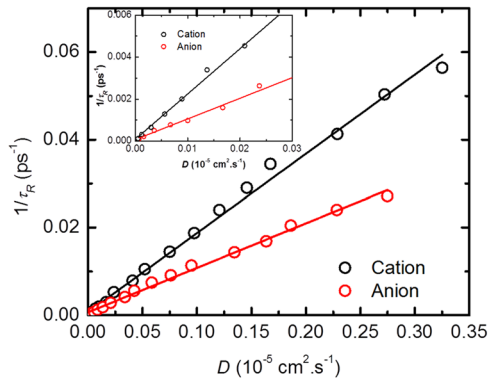

FIG. 10. The linear relationships between the rotational lifetimes and the diffusion coefficients. The inset is the local enlarged area of Fig. 10.

hydrodynamic volume of the cation is ~0.021 nm^3, which is about 9 times smaller than the cation volume value 0.196 nm^3 [62] and 7 times smaller than the cation van der Waals volume 0.142 nm^3.[63] Therefore, the abnormal value of the hydrodynamic volume demonstrates that the IL does not obey the hydrodynamic model. This result agrees with the aforementioned breakdown of the Stokes-Einstein relation. Previous NMR experiments and MD simulations[42,64] also confirmed the breakdown of the hydrodynamic model in IL systems. Due to the similar values and the direct linear relationship between the orientational relaxation decay time and the cage lifetimes (Fig. S8), we can suggest a scenario to account for the transport mechanism in ILs. In IL systems, the cations and anions are surrounded by counterion cages. For an ion to undergo spatial diffusion, it needs to break the ion cage first and then hop from one cage to another cage. However, due to multiple hydrogen bonds and complex interactions between the ion and the counterion cage, directly diffusing from one cage to another is difficult. A possible way to break out a counterion cage is through reorientation. The reorientation of ions is likely to require cleaving the hydrogen bonds among ions and counterions, which has relatively low activation energy to overcome the counterion restrictions. Then, reorientation is a vital step needed to break the ion cage. Recent experiments and simulations support this picture, i.e., angular jumps are connected to the translational dynamics.[65,66] Thus, strong coupling exists between the reorientation dynamics and translational dynamics in the IL systems. This rotational-translational coupling was previously found in supercooled liquids.[67,68]

D. Cage structures

In the MD simulations, the cage jump random walk model depicts the ion diffusion dynamics well. To gain insights into the cage dynamics, it is useful to understand details of the cage structures. In the cage model, the cage radius is the minimum of the radial distribution function (RDF) of the cation-anion. Figure 11(a) displays the temperature dependence of the cation-anion RDFs, $g(r)$. There is little change in the location of the first minimum with increasing temperature. This demonstrates that the radius of the ion cages does not change substantially with temperature. Only a slight decrease in the height of the first peak with increasing temperature is observed. This change in the peak height occurs because of a difference in the average coordination number (CN) of counterions in the ion cages. The coordination number is defined as the number of ions of one charge surrounding an ion of the opposite charge within a distance given by the first minimum of $g(r)$.

We also studied the relationship between the coordination number of the ion cage and the temperature. There is a good linear relation between the coordination number and the temperature, as shown in Fig. S9 of the supplementary material. The result demonstrates a linear temperature dependence of the ion cage microstructure. In this description, the average coordination number of the ion cage determines the ion cage potential energy and directly affects the diffusion dynamics. The electrostatic potential energy is the main contribution to the ion cage potential energy. The ion cage potential energy, E_p, is proportional to the ion cage charges, i.e.,

$$E = \frac{CQ_{cage}q}{4\pi\varepsilon_0 r} = \frac{CN_c q^2}{4\pi\varepsilon_0 r}, \tag{1}$$

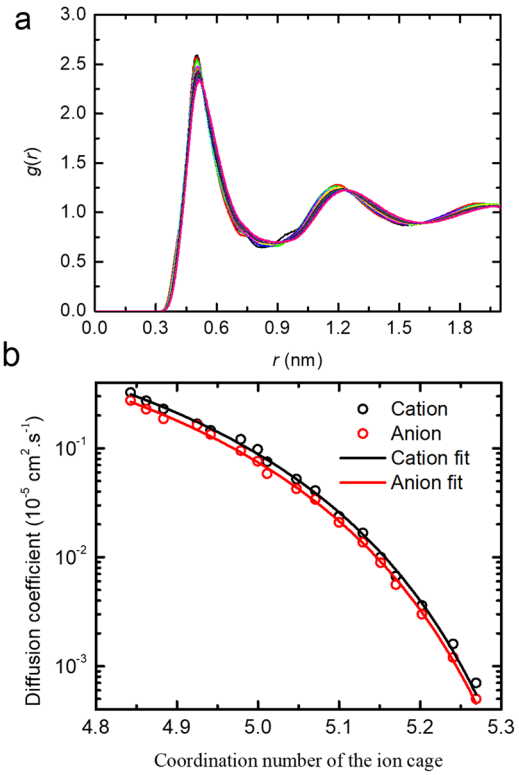

FIG. 11. (a) The temperature-dependent cation-anion radial distribution functions. (b) The fit by Eq. (6) between the coordination numbers of the ion cage and the self-diffusion coefficients for the cation and the anion. The coordination number was calculated by integrating $g(r)$ out to the location of the first minimum.

where q is the charge of the central ion, N_c is the coordination number of the ion cage, r is the cage radius, which corresponds to the location of the minimum in the cation-anion radial distribution function, $g(r)$, and

$$Q_{cage} = N_c q \tag{2}$$

is the charge of the counterion cage. We assume the diffusion dynamics are described by the VFT equation,

$$D = D_0 e^{-\frac{E}{R(T-T_0)}} \tag{3}$$

and r remains constant with increasing temperature [Fig. 11(a)]. Assuming the apparent activation energy E is equal to the ion cage potential energy E_p, and then, we can obtain a relation

$$D = D_0 e^{-\frac{CN_c q^2}{4\pi\varepsilon_0 rR(T-T_0)}} = D_0 e^{\frac{KN_c}{T-T_0}}, \tag{4}$$

where K is a constant. Due to the linear relation between the temperature and the coordination number (see Fig. S9 of the supplementary material),

$$T = c_1 N + c_2, \tag{5}$$

where c_1 and c_2 are constants. Substituting Eq. (5) into Eq. (4) gives

$$D = D_0 e^{\frac{A}{B-\frac{1}{N_c}}}, \quad (6)$$

where A and B are both constant.

Equation (6) is similar to the general VFT equation, but it includes a variation in the coordination number N_c with temperature. Figure 11(b) shows the relationship between the average coordination number of the ion cage and the self-diffusion coefficients of the cation and the anion. The good fit between the coordination number of the ion cage and the diffusion coefficients using Eq. (6) demonstrates that our simple ion cage model correctly captures the essential mechanism of ion transport in IL systems. The results indicate that the dynamic properties of ILs are dominated by the coordination number of the ion cage. A very recent study of the glass formers also suggested that the coordination number of neighbors determines the potential-energy barriers and structural relaxation in the supercooled state.[69]

To further understand the detailed microstructure of the ion cage, we calculated the probability distribution of the ion cage coordination number (CN) at several temperatures. The CNs are obtained by examining particular local structures in the simulation and counting the number of counterions surrounding an ion within the distance given by the first minimum of $g(r)$ [see Fig. 11(a)]. Figure 12 shows that there is a broad ion cage microstructure distribution in $BmimNTf_2$. We fit the probability distribution with a Gaussian distribution function (solid curves). A Gaussian fits the data very well at each temperature. A Gaussian distribution usually originates from many independent random processes. It was also found that the random walk model of cage dynamics was able to describe the diffusion of ions. The Gaussian distribution of coordination numbers may be related to the independent and random jump process of caged ions from one cage to another cage. In the coordination number distribution, ion pairs (CN = 1) and complex ion clusterlike cage structures (CN ≥ 2) are present in the IL system. At 300 K, the distribution is centered at a coordination number of 5. At 240 K, the CN is slightly larger (5.5), and at 400 K, it has decreased somewhat (4.6). The widths of the distributions also change with temperature, becoming narrower as the temperature is increased. The full width at half maximum (FWHM) for 240 K, 300 K, and 400 K is 3.3, 3.8, and 4.0, respectively. Different CNs show that the heterogeneous cage structures range from ion pairs to clusterlike cages composed of as many as 10 ions. However, the probabilities of very large CNs or very small CNs are small. Previous studies demonstrated that ion pairs and ion clusters appeared in the IL systems.[17–20] Margulis and Hu[22] pointed out that ILs have structural heterogeneity like glass-forming liquids.

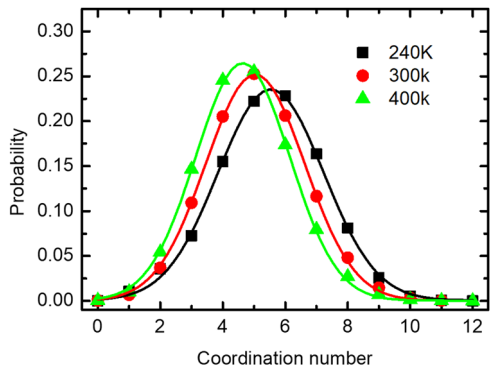

FIG. 12. The detailed probability distribution of the ion cage coordination number at different temperatures. The solid lines are normal Gaussian distribution function fits.

IV. CONCLUDING REMARKS

Ionic liquids have complex cation-anion interactions and diverse microstructures. The various interactions among the cations and the anions, including Coulomb interactions, hydrogen bonding, van der Waals interactions, and dispersion interactions, collectively result in the complex behavior of the transport dynamics in ILs. The Debye-Hückel theory can only explain ion transport in infinitely dilute solutions.[70] In contrast, ILs as electrolytes are composed purely of ions and have complex cation-anion structures ranging from isolated ions[71] to ion pairs and ion clusters. Hence, it remains an important question how the complex range of structures determines the transport behaviors of ILs. Here, we made use of molecular dynamics simulations to investigate the properties of the IL $BmimNTf_2$. It was found that $BmimNTf_2$ exhibits many dynamical properties found in glass-forming liquids, including subdiffusive behavior, breakdown of the Stokes-Einstein relation, and the ability of the VFT equation to describe the temperature dependence of the structural relaxation dynamics, the translational dynamics, and the reorientation dynamics.

We presented an ion cage model to explain these dynamical properties. The ion cage dynamics can be accurately described by the random walk model. Further structural analysis of the ion cages demonstrated that the electrostatic potential energy of the ion cage determines the diffusion dynamics of the central cage ion. We suggested that reorientation of caged ions is a key step for breaking the cage. Strong rotational-translational coupling may be an important general phenomenon in IL systems. We also studied the probability distributions of ion cage coordination numbers at several temperatures. The average coordination number (see Fig. 12) varied from 240 K to 400 K, going from 5.5 to 4.6. Over this temperature range, the FWHM of the distribution narrowed as the temperature increased, going from 4.0 to 3.3. The supercooled liquid like dynamical properties may be ascribed to the distribution of coordination numbers and ion cage structures.

One particularly interesting result to come out of this work is the calculation of the ion cage lifetime and its relationship to the diffusion constant. It was found that a simple random walk diffusion model, using the ion change lifetime as the step time for the random walk, provides an excellent description of the cation and anion spatial diffusion (see Figs. 6 and 7). A recent paper by Feng *et al.*[71] pointed out that the ionic diffusion of ILs involved two states with interstate exchange occurring in a manner somewhat analogous to semiconductors, i.e., in the ILs, there are quasifree ions and bound ions. From our random walk ion cage model and Gaussian ion cage distribution, we know that the ILs have abundant dynamic states and complex interstate exchange that can be described by the random walk model. These different cage cluster sizes inevitably result in a very broad distribution of dynamics time scales, which is also

one of the origins of the dynamic heterogeneity in ILs. Small clusters produce fast ion diffusion; conversely, large clusters can present as quasibound dynamic states, which is the reason that "two states with free and bound state" were observed in ILs.[71] Our subsequent research will focus on the detailed analysis on different size cluster dynamics and the frequency of interstate exchange.

The study presented here also raises a series of questions. Does the ion cage effect dominate the dynamical behavior of all types of ionic liquids, including protic ILs or ILs consisting of very different cation-anion volumes? Of the variety of competing ion interactions that occur in ILs, does one, e.g., Coulomb interactions, determines the ion cage structure or is it determined by the subtle interplay of a variety of interactions? Is it possible to tune the ion cage structures in a systematic manner by choice of ion properties, e.g., cation alkyl chain length, to obtain improved electrolytes with high electrical conductivity? The approach present here, using the cage correlation function to determine the cage lifetime, and relating the cage dynamics to dynamical properties of the liquids, should be useful for other ILs and for addressing some of these important questions.

SUPPLEMENTAL MATERIAL

See the supplementary material for molecular structures of $BmimNTf_2$, comparisons of densities and diffusion coefficients between the MD simulation and experimental results, the temperature dependence of mean square displacement, the temperature dependence of rotational autocorrelation functions, the relationship between the rotational lifetime and the cage lifetime, the linear relationship between the coordination number of the ion cage and the temperature, the VFT fit parameters, and the probability distribution of waiting time in ion cage.

ACKNOWLEDGMENTS

We would like to thank Steven A. Yamada (Stanford University), D. J. Hoffman (Stanford University), Weizhong Zheng (East China University of Science and Technology) for helpful discussions and suggestions. This work was supported by the Project of the Anhui Higher Education Top-notch Talent of China (Grant No. gxgwfx2018066), the Anhui Provincial Natural Science Foundation (Grant Nos. 1808085QE127 and 1808085QE154), the Natural Science Foundation of the Anhui Higher Education Institutions of China (Grant No. KJ2017A930), and Young Teachers Special Project of Hefei Normal University (Grant No. 2017QN16). M.D.F. was supported by the Division of Chemical Sciences, Geosciences, and Biosciences, Office of Basic Energy Sciences of the U.S. Department of Energy through Grant No. DE-FG03-84ER13251.

REFERENCES

[1] R. D. Rogers and K. R. Seddon, "Ionic liquids–solvents of the future?," Science **302**, 792 (2003).
[2] T. Welton, Chem. Rev. **99**, 2071 (1999).
[3] T. L. Greaves and C. J. Drummond, Chem. Rev. **108**, 206 (2008).
[4] N. V. Plechkova and K. R. Seddon, Chem. Soc. Rev. **37**, 123 (2008).
[5] H. Zhao and S. V. Malhotra, Aldrichimica Acta **35**, 75 (2002), available at https://www.sigmaaldrich.com/ifb/acta/v35/HTML/96/index.html.
[6] A. Berthod, M. Ruiz-Angel, and S. Carda-Broch, J. Chromatogra. A **1184**, 6 (2008).
[7] M. C. Buzzeo, R. G. Evans, and R. G. Compton, ChemPhysChem **5**, 1106 (2004).
[8] T. Welton, Coord. Chem. Rev. **248**, 2459 (2004).
[9] M. Galiński, A. Lewandowski, and I. Stępniak, Electrochim. Acta **51**, 5567 (2006).
[10] D. R. MacFarlane, N. Tachikawa, M. Forsyth, J. M. Pringle, P. C. Howlett, G. D. Elliott, J. H. Davis, M. Watanabe, P. Simon, and C. A. Angell, Energy Environ. Sci. **7**, 232 (2014).
[11] J. R. Sangoro and F. Kremer, Acc. Chem. Res. **45**, 525 (2011).
[12] W. Xu and C. A. Angell, Science **302**, 422 (2003).
[13] J. Sangoro, C. Iacob, A. Serghei, S. Naumov, P. Galvosas, J. Kärger, C. Wespe, F. Bordusa, A. Stoppa, and J. Hunger, J. Chem. Phys. **128**, 214509 (2008).
[14] A. Rivera, A. Brodin, A. Pugachev, and E. Rössler, J. Chem. Phys. **126**, 114503 (2007).
[15] M. Klähn, A. Seduraman, and P. Wu, J. Phys. Chem. B **112**, 13849 (2008).
[16] J. Habasaki and K. Ngai, J. Chem. Phys. **129**, 194501 (2008).
[17] W. Zhao, F. Leroy, B. Heggen, S. Zahn, B. Kirchner, S. Balasubramanian, and F. Müller-Plathe, J. Am. Chem. Soc. **131**, 15825 (2009).
[18] H. K. Stassen, R. Ludwig, A. Wulf, and J. Dupont, Chem. Eur. J. **21**, 8324 (2015).
[19] S. Chen, S. Zhang, X. Liu, J. Wang, J. Wang, K. Dong, J. Sun, and B. Xu, Phys. Chem. Chem. Phys. **16**, 5893 (2014).
[20] M. Del Popolo, C. Mullan, J. Holbrey, C. Hardacre, and P. Ballone, J. Am. Chem. Soc. **130**, 7032 (2008).
[21] D. A. Turton, J. Hunger, A. Stoppa, G. Hefter, A. Thoman, M. Walther, R. Buchner, and K. Wynne, J. Am. Chem. Soc. **131**, 11140 (2009).
[22] Z. Hu and C. J. Margulis, Proc. Natl. Acad. Sci. U. S. A. **103**, 831 (2006).
[23] Z. P. Zheng, W. H. Fan, S. Roy, K. Mazur, A. Nazet, R. Buchner, M. Bonn, and J. Hunger, Angew. Chem., Int. Ed. **54**, 687 (2015).
[24] Y. Wang and G. A. Voth, J. Am. Chem. Soc. **127**, 12192 (2005).
[25] M. Sha, Y. Liu, H. Dong, F. Luo, F. Jiang, Z. Tang, G. Zhu, and G. Wu, Soft Matter **12**, 8942 (2016).
[26] M. D. Ediger, Annu. Rev. Phys. Chem. **51**, 99 (2000).
[27] P. Zhang, J. J. Maldonis, Z. Liu, J. Schroers, and P. M. Voyles, Nat. Commun. **9**, 1129 (2018).
[28] P. G. Debenedetti and F. H. Stillinger, Nature **410**, 259 (2001).
[29] R. Torre, P. Bartolini, and R. Righini, Nature **428**, 296 (2004).
[30] J. D. Eaves and D. R. Reichman, Proc. Natl. Acad. Sci. U. S. A. **106**, 15171 (2009).
[31] M. G. Del Pópolo and G. A. Voth, J. Phys. Chem. B **108**, 1744 (2004).
[32] M. Casalegno, G. Raos, G. B. Appetecchi, S. Passerini, F. Castiglione, and A. Mele, J. Phys. Chem. Lett. **8**, 5196 (2017).
[33] M. A. Gebbie, M. Valtiner, X. Banquy, E. T. Fox, W. A. Henderson, and J. N. Israelachvili, Proc. Natl. Acad. Sci. U. S. A. **110**, 9674 (2013).
[34] A. A. Lee, D. Vella, S. Perkin, and A. Goriely, J. Phys. Chem. Lett. **6**, 159 (2014).
[35] S. Perkin, M. Salanne, P. Madden, and R. Lynden-Bell, Proc. Natl. Acad. Sci. U. S. A. **110**, E4121 (2013).
[36] M. Sha, H. Dong, F. Luo, Z. Tang, G. Zhu, and G. Wu, J. Phys. Chem. Lett. **6**, 3713 (2015).
[37] M. Bešter-Rogač, A. Stoppa, J. Hunger, G. Hefter, and R. Buchner, Phys. Chem. Chem. Phys. **13**, 17588 (2011).
[38] A. Knorr, P. Stange, K. Fumino, F. Weinhold, and R. Ludwig, ChemPhysChem **17**, 458 (2016).
[39] Y. Zhang and E. J. Maginn, J. Phys. Chem. Lett. **6**, 700 (2015).
[40] Y. Zhang, L. Xue, F. Khabaz, R. Doerfler, E. L. Quitevis, R. Khare, and E. J. Maginn, J. Phys. Chem. B **119**, 14934 (2015).
[41] T. Köddermann, D. Paschek, and R. Ludwig, ChemPhysChem **8**, 2464 (2007).
[42] T. Köddermann, R. Ludwig, and D. Paschek, ChemPhysChem **9**, 1851 (2008).
[43] J. C. Araque, S. K. Yadav, M. Shadeck, M. Maroncelli, and C. J. Margulis, J. Phys. Chem. B **119**, 7015 (2015).
[44] E. Choi, J. G. McDaniel, J. R. Schmidt, and A. Yethiraj, J. Phys. Chem. Lett. **5**, 2670 (2014).
[45] D. Van Der Spoel, E. Lindahl, B. Hess, G. Groenhof, A. E. Mark, and H. J. Berendsen, J. Comput. Chem. **26**, 1701 (2005).
[46] B. Hess, C. Kutzner, D. Van Der Spoel, and E. Lindahl, J. Chem. Theory Comput. **4**, 435 (2008).

[47]M. J. Abraham, T. Murtola, R. Schulz, S. Páll, J. C. Smith, B. Hess, and E. Lindahl, Software X **1**, 19 (2015).
[48]S. Sastry, P. G. Debenedetti, and F. H. Stillinger, Nature **393**, 554 (1998).
[49]D. N. Perera and P. Harrowell, Phys. Rev. Lett. **81**, 120 (1998).
[50]W. Kob, J. Phys.: Condens. Matter **11**, R85 (1999).
[51]W. Kob and H. C. Andersen, Phys. Rev. Lett. **73**, 1376 (1994).
[52]L. Xu, F. Mallamace, Z. Yan, F. W. Starr, S. V. Buldyrev, and H. E. Stanley, Nat. Phys. **5**, 565 (2009).
[53]C. A. Angell, Science **267**, 1924 (1995).
[54]E. Rabani, J. D. Gezelter, and B. Berne, J. Chem. Phys. **107**(17), 6867 (1997).
[55]J. D. Gezelter, E. Rabani, and B. Berne, J. Chem. Phys. **110**, 3444 (1999).
[56]B. Aoun, M. A. González, J. Ollivier, M. Russina, Z. Izaola, D. L. Price, and M.-L. Saboungi, J. Phys. Chem. Lett. **1**, 2503 (2010).
[57]T. I. Morrow and E. J. Maginn, J. Phys. Chem. B **106**, 12807 (2002).
[58]E. Bertin, J.-P. Bouchaud, and F. Lequeux, Phys. Rev. Lett. **95**, 015702 (2005).
[59]A. Noda, K. Hayamizu, and M. Watanabe, J. Phys. Chem. B **105**, 4603 (2001).
[60]H. Tokuda, K. Ishii, M. A. B. H. Susan, S. Tsuzuki, K. Hayamizu, and M. Watanabe, J. Phys. Chem. B **110**, 2833 (2006).
[61]C. M. Hu and R. Zwanzig, J. Chem. Phys. **60**, 4354 (1974).
[62]U. P. Preiss, J. M. Slattery, and I. Krossing, Ind. Eng. Chem. Res. **48**, 2290 (2009).
[63]W. Beichel, P. Eiden, and I. Krossing, ChemPhysChem **14**, 3221 (2013).
[64]A. Wulf, R. Ludwig, P. Sasisanker, and H. Weingärtner, Chem. Phys. Lett. **439**, 323 (2007).
[65]J. Hunger, T. Sonnleitner, L. Liu, R. Buchner, M. Bonn, and H. J. Bakker, J. Phys. Chem. Lett. **3**, 3034 (2012).
[66]S. Das, B. Mukherjee, and R. Biswas, J. Chem. Phys. **148**, 193839 (2018).
[67]S. H. Chong and W. Kob, Phys. Rev. Lett. **102**, 025702 (2009).
[68]G. Hinze, R. Francis, and M. Fayer, J. Chem. Phys. **111**, 2710 (1999).
[69]A. Singh and Y. Singh, Phys. Rev. E **99**, 030101 (2019).
[70]P. Debye and E. Hückel, Phys. Z. **24**, 185 (1923).
[71]G. Feng, M. Chen, S. Bi, Z. A. Goodwin, E. B. Postnikov, N. Brilliantov, M. Urbakh, and A. A. Kornyshev, Phys. Rev. X **9**, 021024 (2019).